NANO LETTERS

pubs.acs.org/NanoLett

Two-Stage Capture Employing Active Transport Enables Sensitive and Fast Biosensors

Parag Katira, and Henry Hess*

Department of Materials Science and Engineering, University of Florida, Gainesville, Florida 32611-6400

ABSTRACT Nanoscale sensors enable the detection of analytes with improved signal-to-noise ratio but suffer from mass transport limitations. Molecular shuttles, assembled from, e.g., antibody-functionalized microtubules and kinesin motor proteins, can selectively capture analytes from solution and deliver the analytes to a sensor patch. This two-stage process can accelerate mass transport to nanoscale biosensors and facilitate the rapid detection of analytes. Here, the possible increase of the signal-to-noise ratio is calculated, and the optimal layout of a system which integrates active transport is determined.

KEYWORDS Sensor, diffusion, motor protein, molecular shuttle, active transport

One of the applications of nanoscale transport systems, such as molecular shuttles[1,2] and nanocars,[3] is the capture and concentration of biological analytes and their subsequent deposition at a sensing element. The goal of integrating active transport into a sensor platform is enhancing performance (quantified by sensitivity AND response time) by accelerating analyte transport to the sensor, because mass transport constitutes a bottleneck in platforms based on nanoscale sensing elements.[4,5]

The inspiration for this approach is of biological origin, since motor proteins have been found to fulfill diverse transport functions within cells.[6] For example, certain viruses "hijack" motor protein transporters to accelerate their travel from the periphery of the cell to the nucleus.[7,8] Furthermore, a two-stage process of capturing an analyte on a surface followed by surface diffusion to the target site has been shown to be an effective approach to accelerate the interaction of dilute analytes with small target sites in a variety of biological situations.[9]

The pursuit of such a two-stage sensor platform, where analyte capture from solution is followed by a surface transport process, is enabled by the development of nanoscale sensing elements and of molecular shuttles capable of capturing and transporting analytes.[10−14] Here, we calculate the potential payoff of this design and the optimal layout of a platform. We find that the accumulation of analyte at the sensor can be accelerated by several orders of magnitude, which would overcome the mass transfer limitations for nanoscale sensors pointed out by Sheehan and Whitman.[4]

Our argument is organized as follows: We consider a sensor site as it would exist on a microarray chip (Figure 1) and calculate the number of analyte molecules collected at the sensor patch if the analyte molecules reach the sensor patch by three-dimensional (3D) diffusion (Figure 1A), by 3D diffusion to the surface followed by two-dimensional (2D) diffusive transport[15] to the sensor patch (Figure 1B), and

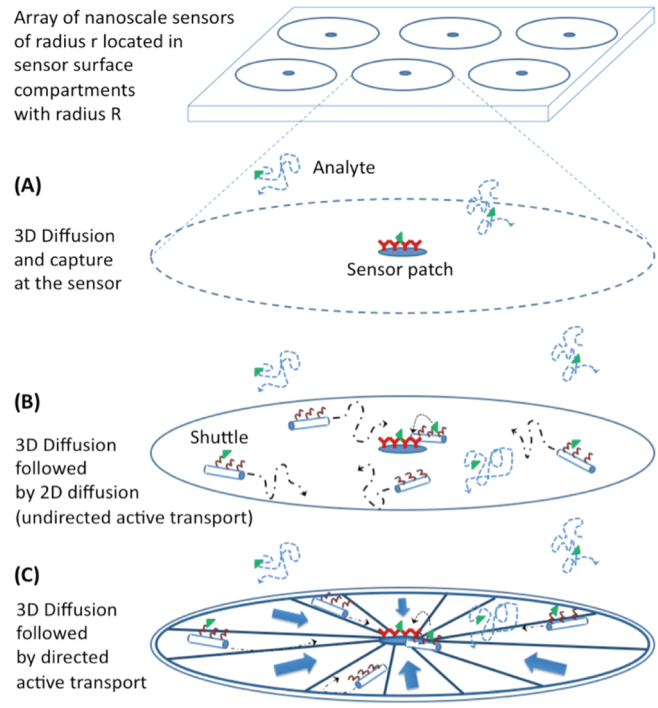

FIGURE 1. A biosensor, such as a microarray, frequently employs multiplexed sensor patches arrayed on a surface. Analytes may reach the sensor patches by (A) conventional 3D diffusion to the sensor patch of radius *r*, or two-stage capture of analytes by surface transporters operating in a compartment with radius *R* and moving to the sensor via (B) diffusive motion or (C) via directed movement along defined tracks.

* To whom correspondence should be addressed. Present address: Columbia University, Department of Biomedical Engineering, 351 L Engineering Terrace, MC 8904, 1210 Amsterdam Ave., New York, NY 10027. Fax: (212) 854-8725. Tel: (212) 854-7749. E-mail: hh2374@columbia.edu.

Received for review: 10/16/2009
Published on Web: 01/07/2010

DOI: 10.1021/nl903468p | *Nano Lett.* **2010,** *10,* 567-572

finally by 3D diffusion to the surface followed by directed transport[16,17] to the sensor patch (Figure 1C). We proceed to discuss the implications for the signal-to-noise ratio of the sensor platform and apply our calculations to published experiments.

Since we are interested in very low analyte concentrations (less than picomolar) and fast response times (less than 30 min available for the collection of analyte), we assume that (1) detection is limited by mass transport and not by the reaction rate between analytes and sensors,[18] (2) dissociation of captured molecules can be neglected, and (3) the saturation of sensors can be neglected. Our discussion thus assumes that during the <30 min available for capture, the capture rate is determined by the steady-state flux of the analyte to the sensor surface.

Single-Stage Analyte Capture. In conventional biosensors, analytes diffuse in 3D until they encounter the sensor and are captured. Under the assumptions stated above, the number of analytes N accumulated on a disk-shaped sensor of radius r can be calculated from the diffusion-limited analyte flux $J_{3D\text{-}r}$

$$\frac{dN}{dt} = J_{3D\text{-}r} \tag{1}$$

The steady-state flux to a disk-shaped sensor in a dilute solution of analytes is $J_{3D\text{-}r} = 4DCr$, where D is the diffusion constant and C is the concentration of the analyte.[19] The number of analytes captured by the sensor patch in time t is then given by

$$N = 4DCrt \tag{2}$$

In current microarrays, the sensor radius varies between 10 and 200 μm and a large number of analyte molecules is rapidly accumulated.[20−22] Unfortunately, the accumulation of analyte onto nanoscale sensors is extremely slow and necessitates collection times of many hours (Figure 2).[4,23] Techniques to increase the analyte flux, e.g., stirring or flow, are effective for sensors larger than 10 μm[21] but are not very effective in increasing the analyte flux to nanoscale sensors.[4] This partially negates the advantages of nanoscale sensors in the size range of 1 μm to 10 nm: a signal enhancement due to the capture of analytes into confined sensor patches,[5,24−28] and a reduction in the background noise due to the reduced area of detection.

Two-Stage Analyte Capture. Adam and Delbrück have shown that a two-stage capture process, where diffusion to a surface is followed by diffusion on the surface to a detection site, can increase the analyte flux to the sensor if the 2D surface diffusion constant is comparable to the 3D diffusion constant and the dissociation rate of analyte from the surface is small compared to the analyte capture rate.[9]

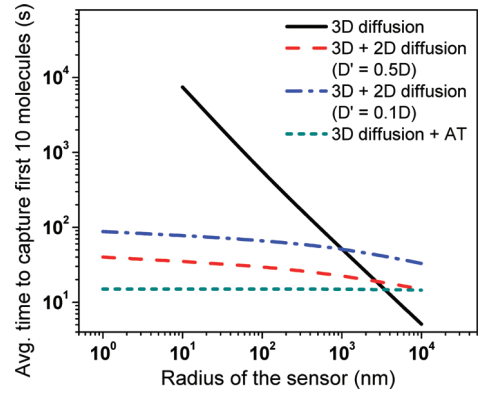

FIGURE 2. Time for capture of first 10 analyte molecules on a disk-shaped sensor of radius r by 3D diffusion, 3D + 2D diffusion and 3D diffusion followed by directed active transport of analyte. We assume a diffusion constant for 3D-diffusion of 80 μm^2/s, 2D-diffusion constant is taken as one-half (∼microtubule diffusion constant on surface) or one-tenth (∼protein diffusion constant in a lipid bilayer) of the 3D-diffusion constant, an analyte concentration C of 1 pM, a compartment radius R of 100 μm, an active transport velocity of 0.5 μm/s, and a capture fraction f of 0.9.

In this situation, the number of analytes N at the sensor patch as a result of the surface transport can be calculated from

$$\frac{dN}{dt} = \frac{N_S}{\tau_{avg}} \tag{3}$$

where N_s is the number of analytes on the surface at time t and τ_{avg} is the average time required for the analyte to find the sensor during the surface diffusion step.

The number of analytes at the surface N_s is determined by the 3D-diffusive flux $J_{3D\text{-}S}$ of analytes to the surface of the sensor and the subsequent 2D-diffusive transport of these analytes to the sensor

$$\frac{dN_S}{dt} = J_{3D\text{-}S} - \frac{N_S}{\tau_{avg}} \tag{4}$$

A two-stage capture process can be facilitated by using molecular transporters that can capture the analytes from solution and transport them from the capture area to the sensor. Since the transporters do not cover the whole surface, the flux of analyte from solution to surface $J_{3D\text{-}S}$ is a fraction f of the steady-state analyte flux to the capture area, which is assumed to be a circular surface compartment of radius R, from solution: $J_{3D\text{-}S} = 4fDCR$. The fraction f is a function of the number of transporters distributed over the compartment surface, but Berg and Purcell[29] have shown that even at low surface coverages it can be close to unity. Solving eqs 3 and 4 with initial conditions $N_S = 0$ at $t = 0$ and $N = 0$ at $t = 0$ yields the number of analytes captured at the sensor

DOI: 10.1021/nl903468p | Nano Lett. 2010, 10, 567-572

$$N = 4fDCR[t - \tau_{avg}(1 - e^{-t/\tau_{avg}})] \quad (5)$$

The average duration of surface transport τ_{avg} depends on the geometry of the surface and sensor and the character of the transport (diffusive or directed). If the sensor patch is located in a circular compartment with radius R and the motion of the analyte transporter on the surface is diffusive, Purcell and Berg[29] have shown that τ_{avg} is given by

$$\tau_{avg} = \frac{R^2}{2D'}\left[\ln\left(\frac{R}{r}\right) - \frac{3}{4}\right] \quad (6)$$

where D' is the surface diffusion constant. If the motion of the analyte transporter is one-dimensional, i.e., directed toward the sensor, then the averaged time for analyte to reach the sensor is given by

$$\tau_{avg} = \frac{L_{avg}}{v} \quad (7)$$

where L_{avg} is the average distance traveled by a transporter to reach the sensor and v is the velocity of surface transport.

Discussion. Molecular shuttles powered by biomolecular motors have been designed based on the microtubule−kinesin or the actin−myosin system.[13,30] A common design for the microtubule−kinesin system is to adhere the kinesin motors to the surface and utilize the immobilized motors to propel microtubules, which serve as the transporter. Specific analytes can be captured and transported by functionalizing the microtubules with antibodies or aptamers.[10,31−34] The path of the gliding microtubules can be controlled by patterning tracks on the surface.[16] Finally, the activity of the motors can be controlled by regulating the supply of the substrate ATP.[35]

On an unpatterned surface, each shuttle moves on a trajectory approximating a wormlike chain.[15,36] Thus, while the trajectory is ballistic over distances much smaller than the trajectory persistence length, over distances larger than the persistence length the path can be described as a 2D random walk with a diffusion constant D' given by $L_p v$, where L_p is the persistence length of the microtubule trajectory.[37] Here, the movement is modeled entirely as a diffusive process, while a more complete treatment might consider diffusive transport to a circular boundary surrounding the sensor patch with radius L_p and ballistic transport inside this boundary.

On a surface patterned with a suitable network of tracks, the microtubule movement can be guided to the sensor patch with a microtubule velocity v. Initially, the microtubules are assumed to be oriented toward and away from the sensor with equal probability, which causes half of them to travel along the track to the periphery of the compartment, reorient, and return.

Molecular shuttles can be integrated into a conventional microarray biosensor (Figure 1B), by replacing each of the spots with a compartment of radius R. The compartment surface can be coated with kinesin, which supports the movement of functionalized microtubules serving as molecular shuttles. These shuttles capture analytes from the solution and transport them to a central nanoscale sensor of radius r.

If there are N_{MT} microtubules on the compartment surface, the diffusion-limited steady-state flux of analytes to the microtubule coated surface is a fraction f of the analyte flux to the whole surface of the compartment (given by $J_{3D\text{-}R} = 4DCR$) with f given by (eq 2.23 and 2.25 in ref 19)

$$f^{-1} = 1 + \frac{2R}{\pi l_{MT} N_{MT}} \ln\left(\frac{2l_{MT}}{d_{MT}}\right) \quad (8)$$

where l_{MT} is the average length of the microtubules and d_{MT} is the diameter of the microtubules. As N_{MT}, the number of shuttles in the compartment, becomes very large, f tends to 1. For a compartment with a radius of 100 μm, a typical density of one shuttle per 100 μm^2 and a microtubule length of 5 μm and width of 25 nm, the fraction of the maximal analyte flux harvested would be 80%.

The number of analytes delivered by the shuttles to the sensor patch can be determined using eq 5. If microtubules move diffusively on an unpatterned surface (Figure 1B, top), the average time to deliver a captured analyte to the sensor patch can be determined from eq 6. The number of analytes accumulated at the sensor is given by

$$N = 4fDCR\left\{t - \frac{R^2}{2L_p v}\left[\ln\left(\frac{R}{r}\right) - \frac{3}{4}\right][1 - e^{-(2L_p vt)/(R^2(\ln(R/r) - 3/4))}]\right\} \quad (9)$$

If shuttles are directly guided to the sensor patch by tracks, the average time to deliver a captured analyte to the sensor is given using eq 7 where $L_{avg} = R - r$. Thus

$$\tau_{avg} = \frac{(R - r)}{v} \quad (10)$$

and eq 5 can be rewritten as

$$N = 4fDCR\left[t - \left(\frac{R - r}{v}\right)(1 - e^{-vt/(R-r)})\right] \quad (11)$$

DOI: 10.1021/nl903468p | Nano Lett. 2010, 10, 567-572

The number of analytes captured in the two-stage capture process using molecular shuttles is plotted for different detection times (15, 30, 60 min) and sensor sizes (radius 1, 10, 100, 1000 nm) in Figures S1 and S2 in Supporting Information. Typical values for analyte diffusion constants as well as shuttle velocities and trajectory persistence lengths have been assumed.

Figure 2 shows that for nanoscale sensor patches a two-stage capture process can significantly accelerate the analyte capture compared to a single-stage 3D diffusion capture process. Furthermore, directed movement of molecular shuttles along tracks provides a relatively small advantage over diffusive movement on an unpatterned surface.

Equations 9 and 11 can be used to optimize the design of the sensor (Figure S2 in Supporting Information). For diffusive shuttle movement on an unpatterned surface, the size of the collection compartment has an optimum at which the number of collected analytes is maximal. This optimal compartment size depends primarily on the time available for detection (Figure S1 in Supporting Information), and it represents a balance between the number of shuttles collecting analytes and the average time needed to reach the sensor. For kinesin-powered molecular shuttles, the optimal radius of the collection compartment is on the order of 100 μm for a 30 min detection window. For directed shuttle movement on a patterned surface, the number of collected analytes increases asymptotically with increasing compartment radius (Figure S2 in Supporting Information). The optimum design parameters are plotted for specific sensor sizes and detection times in Figure S3 in Supporting Information.

Implications for the Signal-to-Noise Ratio. A counterargument to the use of molecular shuttles is that the performance comparison should be made between the molecular shuttle sensor and a diffusion-based sensor of a size equal to the size of the collection compartment. Since the analyte flux to the compartment surface is larger than the analyte flux delivered by the shuttles to the nanoscale sensor patch (see eq 8), the traditional, microscale sensor should actually perform better.

However, the key metric to consider is the signal-to-noise ratio (SNR) of the sensor. Several sources contribute to the noise, including the shot noise of the signal, the noise introduced by a background signal, and the noise introduced by the detection system. A reduction in the size of the sensor patch is often accompanied by a corresponding reduction in the size of the background signal, which improves the SNR if all other contributions are unchanged.

For example, in fluorescence imaging a reduction in the illuminated area is accompanied by a reduction in the illumination of out-of-focus planes with a concomitant decrease in the fluorescence background and its accompanying noise term. Similarly, problems with cross-reactivity and nonspecific adsorption may be reduced for a smaller sensor.

In summary, the SNR is increased for a sensor device integrating active transport if the small loss in the number of collected analytes is overcompensated by a large reduction in the background signal or if the noise introduced by the signal transduction mechanism in the sensor is significantly reduced as a result of the miniaturization to the nanoscale.[38]

Application of the Model. The above-described analysis can be applied to two experimental systems recently described in the literature. The sensor design by Lin et al. employs capture of analytes in a compartment (radius ~90 μm) onto microtubules followed by directed transport into the sensor area (radius ~10 μm).[11] Assuming an initial microtubule density within the compartment of 0.05 μm^{-2} and an average microtubule length of 5 μm, eq 8 yields $f =$ 0.95. In this system, the microtubules are stationary while capturing analytes for 1 min. Then the analyte solution is replaced with a motility solution that triggers microtubule movement. After a collection period of 14 min, all of the microtubules have reached the sensor area.

At a typical analyte concentration studied by Lin et al., e.g., 1 pM, approximately 1000 analytes would be captured at the sensor patch. Although the sensor design by Lin et al. does provide the proof of principle of a two-stage capture biosensor, it is not yet optimized for an increased SNR. In fact, 3D diffusion based capture of 1 pM streptavidin at the sensor with 10 μm radius would result in approximately 1700 captured molecules. The sensor design utilized by Lin et al. can be modeled by modifying eq 11 to incorporate analyte capture by stationary microtubules followed by directed transport toward sensor, which yields

$$N = 4fDCR[t - t_{AT}][1 - e^{-vt_{AT}/(R-r)}] \qquad (12)$$

where t_{AT} is the time for which the microtubules are actively transported toward the sensing area. The optimum design for this setup and 15 min detection time is 11 min for analyte capture and 4 min of active transport and yields 8000 captured molecules.

Fischer et al.[12] developed a two-stage sensor design where the shuttles capture the analyte in the center of a circular well and deliver it in a diffusive motion to the sensor periphery for detection. If the density of shuttles is high enough at all times, changes in f can be neglected and eq 5 can be applied to this design, even though the shuttle density decreases over time. As the captured analytes are transported to the periphery rather than the center, the average transport time in this case is given by

$$\tau_{avg} = \frac{R^2}{8D'} \qquad (13)$$

where, $D' = L_p v$ with L_p being the trajectory persistence length and v the velocity of the shuttle.[37] For a detection time

DOI: 10.1021/nl903468p | Nano Lett. 2010, 10, 567-572

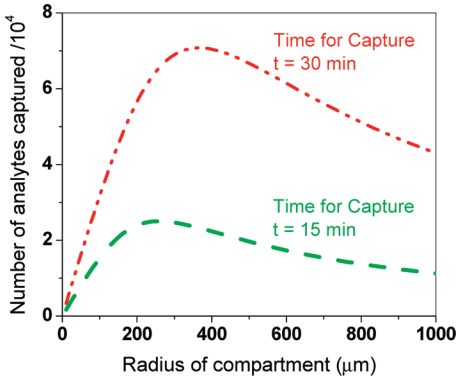

FIGURE 3. Analyte capture as function of compartment size for a sensor integrating active transport of the type described by Fischer et al.[12] A microtubule trajectory persistence length of $L_p = 100\ \mu$m, a gliding velocity of $v = 200$ nm/s, an analyte concentration of 1 pM, and a diffusion constant of 80 μm^2/s were assumed.

of 30 min as desired by Fischer et al., the optimum compartment radius is 375 μm (Figure 3), while a radius of 400 μm was employed. However, if even shorter detection times are desired (e.g., 15 min), this radius should be smaller (250 μm).

Conclusion. As Adam, Berg, and Delbrück recognized 4 decades ago, the scaling of diffusion processes to the nanoscale has nonobvious consequences and enables distinct approaches to the capture and detection of molecular analytes. A careful evaluation of the combination of diffusive transport with novel active transport mechanisms, such as molecular shuttles, demonstrates that analyte capture can be accelerated by orders of magnitude if the system is suitably designed. Furthermore, the analysis can be applied to transporters under development, such as nanocars,[3] to define the benchmarks these transport systems have to meet to be advantageously employed in a sensor system.

Of course, the presented analysis of the mass transport situation does not capture the full complexity of sensor systems. For example, nonspecific and adventitious adsorption of analytes to the surface[39] or the complex nature of the analyte−shuttle interaction[40] may complicate the picture. However, an accounting of diffusion and active transport are the foundation of rational sensor design.

Acknowledgment. Financial support from the DARPA Biomolecular Motors Program (AFOSR FA9550-05-1-0274 and FA9550-05-1-0366) and the University of Florida (UF) Center for Sensor Materials and Technologies (ONR N00014-07-1-0982) is gratefully acknowledged.

Supporting Information Available. Figures showing number of analytes collected for analyte diffusion as a function of compartment radius and optimum compartment size for a two-stage capture process. This material is available free of charge via the Internet at http://pubs.acs.org.

REFERENCES AND NOTES

(1) Nicolau, D. V.; Suzuki, H.; Mashiko, S.; Taguchi, T.; Yoshikawa, S. *Biophys. J.* **1999**, *77* (2), 1126–34.
(2) Hess, H.; Clemmens, J.; Qin, D.; Howard, J.; Vogel, V. *Nano Lett.* **2001**, *1* (5), 235–239.
(3) Shirai, Y.; Osgood, A. J.; Zhao, Y. M.; Kelly, K. F.; Tour, J. M. *Nano Lett.* **2005**, *5* (11), 2330–2334.
(4) Sheehan, P. E.; Whitman, L. J. *Nano Lett.* **2005**, *5* (4), 803–807.
(5) Gooding, J. J. *Small* **2006**, *2* (3), 313–315.
(6) Schliwa, M.; Woehlke, G. *Nature* **2003**, *422* (6933), 759–65.
(7) Campbell, E. M.; Hope, T. J. *Adv. Drug Delivery Rev.* **2003**, *55* (6), 761–71.
(8) Radtke, K.; Dohner, K.; Sodeik, B. *Cell. Microbiol.* **2006**, *8* (3), 387–400.
(9) Adam, G.; Delbrück, M., Reduction of Dimensionality in Biological Diffusion Processes. In *Structural Chemistry and Molecular Biology*; Rich, A., Davidson, N. , Eds.; W. H. Freeman and Co.: New York, 1968; pp 198−215.
(10) Ramachandran, S.; Ernst, K.-H.; Bachand, George D.; Vogel, V.; Hess, H. *Small* **2006**, *2* (3), 330–334.
(11) Lin, C. T.; Kao, M. T.; Kurabayashi, K.; Meyhofer, E. *Nano Lett.* **2008**, *8* (4), 1041–1046.
(12) Fischer, T.; Agarwal, A.; Hess, H. *Nat. Nanotechnol.* **2009**, *4*, 162–166.
(13) Mansson, A.; Sundberg, M.; Bunk, R.; Balaz, M.; Nicholls, I. A.; Omling, P.; Tegenfeldt, J. O.; Tagerud, S.; Montelius, L. *IEEE Trans. Adv/ Packag.* **2005**, *28* (4), 547–555.
(14) Agarwal, A.; Hess, H. *Prog. Polym. Sci.* In Press.
(15) Nitta, T.; Hess, H. *Nano Lett.* **2005**, *5* (7), 1337–1342.
(16) Hiratsuka, Y.; Tada, T.; Oiwa, K.; Kanayama, T.; Uyeda, T. Q. *Biophys. J.* **2001**, *81* (3), 1555–61.
(17) Hess, H.; Clemmens, J.; Matzke, C. M.; Bachand, G. D.; Bunker, B. C.; Vogel, V. *Appl. Phys. A: Mater. Sci. Process.* **2002**, *75*, 309–313.
(18) Squires, T. M.; Messinger, R. J.; Manalis, S. R. *Nat. Biotechnol.* **2008**, *26* (4), 417–426.
(19) Berg, H. C., *Random walks in biology*. Princeton University Press: Princeton, NJ, 1983; p ix, 142 p.
(20) Heller, M. J. *Annu. Rev. Biomed. Eng.* **2002**, *4*, 129–153.
(21) Kusnezow, W.; Syagailo, Y. V.; Ruffer, S.; Baudenstiel, N.; Gauer, C.; Hoheisel, J. D.; Wild, D.; Goychuk, I. *Mol. Cell. Proteomics* **2006**, *5* (9), 1681–1696.
(22) Vail, T. L.; Cushing, K. W.; Ingram, J. C.; Omer, I. S. *Biotechnol. Appl. Biochem.* **2006**, *43*, 85–91.
(23) Bishop, J.; Chagovetz, A.; Blair, S. *Nanotechnology* **2006**, *17* (10), 2442–2448.
(24) Schmidt, J. J.; Montemagno, C. D. *Annu. Rev. Mater. Res.* **2004**, *34*, 315–337.
(25) Brolo, A. G.; Kwok, S. C.; Cooper, M. D.; Moffitt, M. G.; Wang, C. W.; Gordon, R.; Riordon, J.; Kavanagh, K. L. *J. Phys. Chem. B* **2006**, *110* (16), 8307–8313.
(26) Tetz, K. A.; Pang, L.; Fainman, Y. *Opt. Lett.* **2006**, *31* (10), 1528–1530.
(27) Stern, E.; Klemic, J. F.; Routenberg, D. A.; Wyrembak, P. N.; Turner-Evans, D. B.; Hamilton, A. D.; LaVan, D. A.; Fahmy, T. M.; Reed, M. A. *Nature* **2007**, *445* (7127), 519–522.
(28) Senesac, L.; Thundat, T. G. *Mater. Today* **2008**, *11* (3), 28–36.
(29) Berg, H. C.; Purcell, E. M. *Biophys. J.* **1977**, *20* (2), 193–219.
(30) Hess, H.; Vogel, V. *Rev. Mol. Biotechnol.* **2001**, *82* (1), 67–85.
(31) Hirabayashi, M.; Taira, S.; Kobayashi, S.; Konishi, K.; Katoh, K.; Hiratsuka, Y.; Kodaka, M.; Uyeda, T. Q. P.; Yumoto, N.; Kubo, T. *Biotechnol. Bioeng.* **2006**, *94* (3), 473–480.
(32) Taira, S.; Du, Y. Z.; Hiratsuka, Y.; Konishi, K.; Kubo, T.; Uyeda, T. Q. P.; Yumoto, N.; Kodaka, M. *Biotechnol. Bioeng.* **2006**, *95* (3), 533–538.
(33) Bachand, George D.; Rivera, Susan B.; Carroll-Portillo, A.; Hess, H.; Bachand, M. *Small* **2006**, *2* (3), 381–385.

DOI: 10.1021/nl903468p | *Nano Lett.* **2010,** *10,* 567-572

(34) Raab, M.; Hancock, W. O. *Biotechnol. Bioeng.* **2008**, *99* (4), 764–773.
(35) Wu, D.; Tucker, R.; Hess, H. *IEEE Trans. Adv. Packag.* **2005**, *28* (4), 594–599.
(36) Nitta, T.; Tanahashi, A.; Obara, Y.; Hirano, M.; Razumova, M.; Regnier, M.; Hess, H. *Nano Lett.* **2008**, *8* (8), 2305–2309.
(37) Vikhorev, P. G.; Vikhoreva, N. N.; Sundberg, M.; Balaz, M.; Albet-Torres, N.; Bunk, R.; Kvennefors, A.; Liljesson, K.; Nicholls, I. A.; Nilsson, L.; Omling, P.; Tagerud, S.; Montelius, L.; Mansson, A. *Langmuir* **2008**, *24* (23), 13509–13517.
(38) Liu, Y. D.; Mahdavi, F.; Blair, S. *IEEE J. Sel. Top. Quantum Electron.* **2005**, *11* (4), 778–784.
(39) Hucknall, A.; Kim, D.-H.; Rangarajan, S.; Hill, R. T.; Reichert, W. M.; Chilkoti, A. *Adv. Mater.* **2009**, *21* (19), 1968–1971.
(40) Agarwal, A.; Katira, P.; Hess, H. *Nano Lett.* **2009**, *9* (3), 1170–1175.

DOI: 10.1021/nl903468p | *Nano Lett.* **2010,** *10,* 567-572